Saudi Pharmaceutical Journal 28 (2020) 550–559

Contents lists available at ScienceDirect

Saudi Pharmaceutical Journal

journal homepage: www.sciencedirect.com

Original article

Bioassay-guided isolation of anti-hepatitis B virus flavonoid myricetin-3-*O*-rhamnoside along with quercetin from *Guiera senegalensis* leaves

Mohammad K. Parvez [a,*], Mohammed S. Al-Dosari [a,*], Ahmed H. Arbab [a,b], Adnan J. Al-Rehaily [a], Mazin A. S. Abdelwahid [c]

[a] Department of Pharmacognosy, College of Pharmacy, King Saud University, Riyadh, Saudi Arabia
[b] Department of Pharmacognosy, Faculty of Pharmacy, University of Khartoum, Khartoum, Sudan
[c] Department of Pharmaceutical Chemistry, Al-Neelain University, Khartoum, Sudan

ARTICLE INFO

Article history:
Received 16 September 2019
Accepted 11 March 2020
Available online 19 March 2020

Keywords:
Guiera senegalensis
Myricetin-3-*O*-rhamnoside
Quercetin
Hepatitis B virus
anti-HBV

ABSTRACT

Recently, we have shown *in vitro* anti-hepatitis B virus (HBV) activity of *G. senegalensis* J.F. Gmel leaves, and Identified quercetin and other flavonoids by HPTLC. Here we report bioassay-directed fractionation of *G. senegalensis* leaves using column chromatography and isolation of two flavonoinds from the *n*-butanol fraction, their structure determination (^{1}H NMR, ^{13}C NMR and 2D-NMR) and assessment of antiviral activities (HBsAg and HBeAg assay) in HBV-reporter HepG2.2.2.15 cells. Further molecular docking was performed against HBV polymerase (Pol/RT) and capsid (Core) proteins as well as host-receptor sodium taurocholate co-transporting polypeptide (NTCP). The two isolated bioactive compounds were identified as quercetin and myricetin-3-*O*-rhamnoside. Quercetin significantly inhibited synthesis of HBsAg and HBeAg by about 60% and 62%, respectively as compared to myricetin-3-*O*-rhamnoside by 44% and 35%, respectively. Molecular docking of the two anti-HBV flavonoids revealed their higher binding affinities towards Pol/RT than Core and NTCP. In conclusion, this is the first report on anti-HBV active myricetin-3-*O*-rhamnoside along with quercetin isolated from *G. senegalensis* leaves. Their possible mode of anti-HBV activities are suggested through binding with viral Pol/RT and Core as well as host NTCP proteins.

1. Introduction

Hepatitis B virus (HBV) causes acute and chronic hepatitis B that may progress to severe liver diseases (Hou et al., 2005; Shepard et al., 2006). Of over 240 million chronic cases, 15–40% develops fulminant liver failure, cirrhosis or hepatocarcinoma (Tang et al., 2018). Though a DNA virus, HBV very uniquely replicates *via* an RNA intermediate using its polymerase/reverse-tran scriptase (Pol/RT) similar to human immunodeficiency virus (HIV) and herpes simplex virus (HSV). Therefore, most of the anti-HIV/HSV nucleoside analogs (NA) targeting viral Pol/RT are also accepted as effective anti-HBV drugs. However, NA like, lamivudine, adefovir and entecavir are potentially associated with drug-resistance due to emergence of viral Pol/RT mutants, serious clinical problems (Devi and Locarnini, 2013). In recent times, several natural or phytoproducts with equal or even better anti-HBV efficacies have gained global popularity and endorsement (Parvez et al., 2016). A range of plant secondary metabolites including flavonoids, terpenoids, alkaloids, polyphenolics, saponins and lignans has been reported for their promising *in vitro* and *in vivo* anti-HBV activities (Wang et al., 2012; Wu 2016; Parvez et al., 2016; Arbab et al., 2017; Parvez et al., 2019). These anti-HBV compounds differ in their origin, chemistry, potency and type of inhibitory mechanisms, and therefore, their further biological and pharmacological evaluations are warranted.

The African medicinal plant *Guiera senegalensis* J.F. Gmel (family: Combrataceae), commonly known as 'Cure all' is widely used to treat bacterial and fungal infections, gastrointestinal and respiratory disorders as well as malaria (Bosisio et al., 1997; Sanogo et al., 1998; Abubakar et al., 2000; Silva and Gomes, 2003;

* Corresponding authors at: Department of Pharmacognosy, College of Pharmacy, King Saud University, Riyadh 11451, Saudi Arabia.
E-mail addresses: mohkhalid@ksu.edu.sa (M.K. Parvez), mdosari@ksu.edu.sa (M.S. Al-Dosari).
Peer review under responsibility of King Saud University.

Production and hosting by Elsevier

https://doi.org/10.1016/j.jsps.2020.03.006
1319-0164/

Somboro et al., 2011; Akuodor et al., 2013; Suleiman, 2015). Its galls and leaves extracts are shown to have *in vitro* anti-oxidative and anti-inflammatory activities (Bouchet and Barrier, 1998; Sombié et al., 2011; Parvez et al., 2018). Notably, *G. senegalensis* has been also reported to inhibit fowl pox virus (FPV) (Lamien et al., 2005) and HSV (Silva et al., 1997) replications *in vitro*. Recently, in our *in vitro* screening of several medicinal plants extracts against HBV, *G. senegalensis* has demonstrated the best antiviral activity (Arbab et al., 2017). Previously, flavonoids like rutin, quercetin and myricitrin (myricetin-3-*O*-rhamnoside) are isolated from *G. senegalensis* (Bucar et al., 1996; Ficarra et al., 1997; Males et al., 1998). We have recently identified quercetin, rutin, naringenin, gallic acid β-amyrin, β-sitosterol, lupeol and ursolic acid by high-performance thin layer liquid chromatography (HPTLC) method in anti-HBV active *G. senegalensis* leaves extract (Alam et al., 2017; Parvez et al., 2018). Very recently, myricetin, myricitrin and quercetin along with (-)-gallocatechin, 1,3,4,5-tetra-O-galloylquinic acid, gallic acid, methyl gallate, and ethyl gallate isolated from *G. senegalensis* have shown free-radical scavanging, α-glucosidase inhibitory and pancreatic lipase inhibitory activities (Dirar et al., 2019). These results therefore, convincingly prompted us to isolate anti-HBV active principles from *G. senegalensis* leaves. The present study therefore, reports column-guided isolation and structural determination of two anti-HBV compounds from *G. senegalensis* using HBV-reporter cell culture model as well as elucidation of mode of action by molecular docking.

2. Materials and methods

2.1. Plant material

Leaves of *G. senegalensis*, locally known as Gubeish were collected in March 2015 from Kordofan state, Sudan. It was authenticated by a plant taxonomist (Prof. Ismail Mirghani) at the Forestry Research Center (FRC), Khartoum, Sudan, where a voucher specimen (No. 891) was deposited.

2.2. Isolation and characterization of compounds

The dried leaves (450 g) of *G. senegalensis* were ground and extracted with 96% ethanol (Merk, Germany) at room temperature (RT) for 72 h (3×24). After concentrating under vacuum at reduced pressure, the ethanol-extract (38.0 g) was partitioned with *n*-hexane, chloroform and *n*-butanol (all from Merk, Germany) to furnish hexane (4.5 g), chloroform (6.1 g) and *n*-butanol (8.3 g) extracts. Based on the anti-HBV bioassay results (Arbab et al., 2017), the *n*-butanol fraction was subjected to normal phase silica-gel (SiO_2) column chromatography using chloroform:methanol elution with increasing polarity. Of the obtained eight fractions (BF1-BF8), BF2, BF7 and BF8 were associated with anti-HBV activity. Fraction BF2 was subjected to column (Sephadex LH-20) elution with methanol:water (9:1; v/v), giving compound **1** (12.0 mg). It purity was further analyzed by reverse-phase thin layer chromatography (TLC; RP-18 F254 plates; 0.25 mm, Merck, Germany) using mobile phase methanol:water (6:4, v/v) and the spot was visualized by spraying with *p*-anisaldehyde with gentle heating. Fractions BF7 and BF8 were pooled together on the basis of TLC pattern, and chromatographed (Sephadex LH-20) and eluted with methanol:water mixtures of increasing polarity to furnish nine sub-fractions (BSF1-BSF9). Majority of bioactive sub-fractions showing similar TLC profile were combined and re-chromatographed that yielded compound **2** (165.0 mg). Structural characterizations of the isolated compounds **1** and **2** were performed by ^{1}H NMR, ^{13}C NMR and 2D-NMR spectral analyses on a Bruker Avance spectrometer operating at 700 MHz for 1H and 175 for ^{13}C in methanold_4 (Merk, Germany), equipped with a 5 mm cryoprobe using standard pulse programs. The ESI-HRMS were measured on Agilent Technologies 6200 series mass spectrometer.

2.3. Cell culture, compounds and drug

The HBV-reporter human hepatoma cells (kind gift from Dr. S. Jameel, International Center for Genetic engineering & Biotechnology, New Delhi, India) were maintained in RPMI-1640 medium (Gibco, USA), supplemented with heat-inactivated calf serum (10%; Gibco, USA), penicillin-streptomycin (1x; Invitrogen, USA), and sodium pyruvate (1x; Invitrogen, USA) at 37 ^{0}C with 5% CO_2 supply. For all experiments, HepG2.2.2.15 cells (0.5×10^5/100 µl/well) were seeded in 96-well flat-bottom culture plates (Corning, USA), and grown overnight. Stocks of compounds **1** and **2** (1 mg, each) were prepared by first dissolving in 50 µl of dimethyl sulfoxide (DMSO, Sigma, Germany), and then in complete medium (1 mg/ml, final) followed by reconstitution of four different working concentrations (doses: 6.25, 12.5, 25.0 and 50.0 µg/ml). Lamivudine (3TC; Sigma, USA), the standard anti-HBV drug (0.2 µM) and DMSO (0.1%) served as positive and negative/untreated control, respectively. All tests were performed with triplicated samples including controls, and were repeated twice for reproducibility.

2.4. Cell viability assay

The isolated compounds **1** and **2** were first tested on HepG2.2.2.15 for their effects on cells viability (TACS MTT Cell proliferation Assay; Tervigen, USA) as described elsewhere (Arbab et al., 2017). Briefly, cells were treated with the four doses of the compounds and incubated for 24 h. The MTT (3-(4,5-Dimethylthiazol-2-yl)-2,5-diphenyltetrazolium bromide) solution (10 µl/well) was added and incubated at 37 °C for ~5 h until purple color appeared. The detergent solution (100 µl/well) was immediately added and the plate was incubated for another 1.5 h in dark at RT. The absorbance (A; λ = 570 nm) was recorded using microplate reader (Microplate Reader ELx800; BioTek, USA). The data were analyzed to determine cell viability (%) in relation to untreated control $[(As - Ab)/(Ac - Ab)\text{x } 100$; where *As*, *Ab* and *Ac* were the absorbance of sample, blank and negative control, respectively, and presented (Excel software, Microsoft, USA).

2.5. Dose-dependent HBsAg inhibition assay

The anti-HBV activities of compounds **1** and **2** on inhibition of viral HBsAg production in cultured HepG2.2.2.15 cells were evaluated as described elsewhere (Arbab et al., 2017; Parvez et al., 2019). Briefly, cells were treated with the fresh media containing 150 µl of various doses of **1** and **2** including controls for 3 days, and assayed for HBsAg expression (Monolisa HBsAg ULTRA, BioRad, USA) as per the kit's manual. The absorbance was recorded (Microplate Reader ELx800; BioTek, USA) and data was analyzed to estimate inhibition of HBsAg in relation to untreated control.

2.6. Time-course HBeAg inhibition assay

Compounds **1** and **2** at 50 µg/ml dose showing maximal inhibition of HBsAg were further subjected to time-course (day1, 3 and 5) analysis of HBeAg expression, the hallmark of HBV DNA replication (HBeAg/Anti-HBe Elisa Kit (DIASource, Belgium) as per the kit's manual. The absorbance was recorded as above and data was analyzed to estimate inhibition of HBeAg in relation to untreated control.

2.7. In silico molecular docking analysis

To elucidate the anti-HBV modes of action and to determine the molecular interaction patterns, the anti-HBV active compounds **1** (quercetin) and **2** (myricetin-3-*O*-rhamnoside) were docked with two viral proteins HBV-Pol/RT and HBV-Capsid (Core) as well as a host-encoded receptor sodium taurocholate co-transporting polypeptide (NTCP), reported for its binding with HBV envelope (surface) protein (Nakabori et al., 2016). The standard antiviral drug lamivudine and co-crystallized ligand heteroarylpyrimidine (HAP) were used as positive controls against Pol/RT and Core, respectively. While the crystallographic structure for HBV-Core (PDB code: 4 g93) was retrieved from Protein Data Bank (https://www.rcsb.org/), the 3D structures of Pol/RT and NTCP were constructed by comparative homology modeling using SwissModel (Parvez et al., 2019; Waterhouse et al., 2018). The primary sequence of NTCP was retrieved from the protein database (NCBI) and each ligand structure was imported from the PubChem database (https://pubchem.ncbi.nlm.nih.gov/). Solvent molecules and co-crystallized ligands were removed from the proteins and hydrogen atoms were added. The active-site was determined using the SiteFinder program embedded in Molecular Operating Environment (MOE, 2009). Preparation and energy minimization of each protein was performed with MOE (MMFF94 force field; gradient 0.01 kcal/mol Å2). The compound set was docked on the previous target's binding sites by using MOE (Triangle Matcher Method for placement and London dG for scoring). The docking experiment was carried out between the energy-minimized ligands and the active-sites as determined by SiteFinder. The docking poses were ranked according to their docking scores and the results were exported for further analysis. The interactions of the ligands on the targets were visualized and the figures were created by using AutoDoc Vina software in PyRx (Trott and Olson, 2010; Mühlberg et al., 2009).

2.8. Statistical analysis

Data of all triplicated samples were expressed as mean ± S.E.M. Total variation present in a set of data was estimated by one-way analysis of variance (ANOVA) followed by Dunnet's-test (Excel 2010; Microsoft OK, USA). $P < 0.01$ was considered significant.

3. Results

3.1. Isolation of two flavonoids from G. Senegalensis

The two isolated compounds **1** and **2** from *G. senegalensis* *n*-butanol fraction were identified as known flavonoids quercetin and myricetin-3-*O*-rhamnoside, respectively (Suppl. materials) as characterized by their spectral properties.

Compound **1**: ^{1}H NMR: δ_H 6.198 (1H, s, Ar-*H*), 6.40 (1H, s, Ar-H), 6.89 (1H, d, *J* = 8.4 Hz, Ar-H), 7.65 (1H, d, *J* = 8.4 Hz, Ar-*H*), 7.75 (1H, s, Ar-H). ^{13}C NMR: δ_c (ppm): 92.98, 97.80, 103.10, 114.56, 114.80, 120.26, 122.73, 135.83, 144.80, 146.56, 147.35, 156.80, 161.10, 164.15, 175.91 (Ar-C).

The ^{1}H NMR spectrum of compound **1** in CH_3OD exhibited five peaks resonating between δ 6.00 and 8.00 ppm integrated to five protons and confirming the presence of five aromatic protons. These peaks are assignable to: (i) three isolated proton at δ_H 6.198 (1H, s, H-6), 6.403 (1H, s, H-8) and 7.753 (1H, s, H-6′), (ii) two protons at δ_H 6.895 (1H, d, *J* = 8.4 Hz, H-5′) and 7.653 (1H, d, *J* = 8.4 Hz, H-6′). These two latter protons were coupled to each other (*J* = 8.4 Hz, *ortho* coupling). In addition, the ^{13}C NMR spectrum of compound **1** exhibited 15 sp2-hybridized carbons between δ_c 90 and 175 ppm. Among these 15, five carbons were identified as methine carbons while the remaining were quaternary ones according to the DEPT spectrum. Furthermore, The HSQC and HMBC spectra showed the connectivity between the protons and the carbons, which were in complete agreement with the structure of quercetin (Fig. 1) (Agrawal, 1989).

Compound **2**: ^{1}H NMR – CH_3OD: δ_H ppm 0.985 (3H, d, *J* = 5.6 Hz, —*CH*$_3$), 3.394 (1H, —*CH*—), 3.554 (1H, —*CH*—), 3.831 (1H, —*CH*—), 4.270 (1H, —*CH*—), 5.332 (1H, —*CH*—), 6.200 (1H, s, Ar-*H*), 6.362 (1H, s, Ar-*H*), 6.972 (2H, s, Ar-*H*). ^{13}C NMR – *CH*$_3$*OD* δ_c (ppm): 16.30, 70.47, 70.64, 70.70, 71.94, 93.29, 98.38, 102.19, 104.42, 108.14, 120.45, 134.89, 136.45, 145.38, 157.03, 158.01, 161.72, 164.41, 178.20.

The ^{1}H NMR spectrum of compound **2** exhibited nine peaks integrated to twelve protons. The spectrum showed a doublet resonating at δ_H 0.985 (3H, d, *J* = 5.6 Hz, —*CH*$_3$, H-6″) integrated to three which was attributed to a methyl group. Three signals centered at δ_H 6.200 (1H, s, Ar-*H*, H-6), 6.362 (1H, s, Ar-*H*, H-8) and 6.972 (2H, s, Ar-*H*, H-2′ and H-6′) of which the first two was inte-

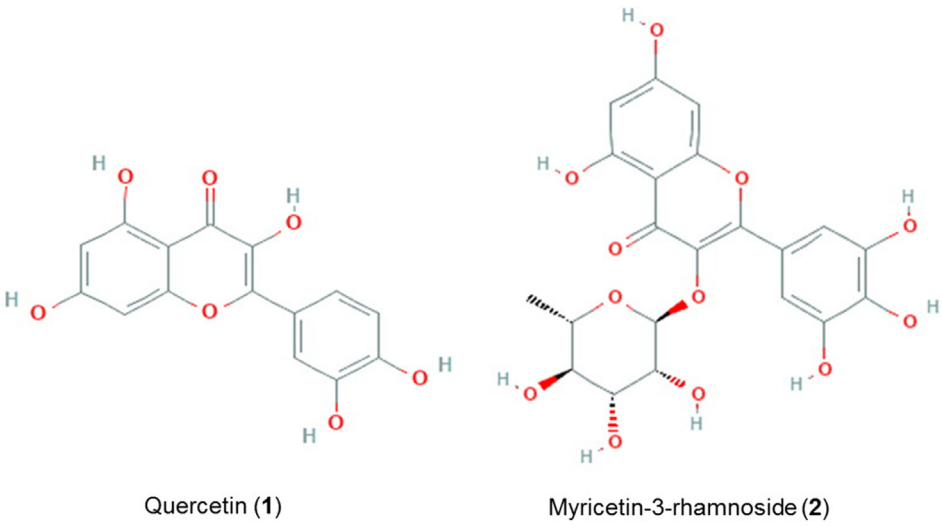

Fig. 1. 2D structures of compounds **1** (quercetin) and **2** (myricetin-3-*O*-rhamnoside) isolated from *G. senegalensis*.

grated into one proton for each, while the latter was integrated into two protons. These three signals ascribed to four isolated aromatic hydrogens were in complete agreement with the known structure of myricetin-3-*O*-rhamnoside (Fig. 1). The most deshielded signal in the aliphatic region of the spectrum was resonating at δ_H 5.332 (1H, —*CH*—, H-1″) and assigned for the protons of anomeric carbon. The remaining peaks resonated between δ_H 3.00 and 4.50 and were ascribable to the protons of the rhamnose carbons. The DEPT spectrum revealed eleven carbons were not linked to hydrogen atoms directly. Finally, the HSQC and HMBC spectra showed the correlation between the protons and the carbons which affirmed the chemical structure of compound 2 that was in complete agreement with the known structure of myricetin-3-0-rhamnoside (Fig. 1) (Agrawal, 1989).

3.2. Non-cytotoxicity of G. Senegalensis derived quercetin and myricetin-3-O-rhamnoside

The isolated (quercetin and myricetin-3-rhamnoside) used up to 50 μg/ml concentration, showed no signs of HepG2.2.2.15 cytotoxicity (Fig. 2). Notably, as compared to quercetin, myricetin-3-*O*-rhamnoside enhanced cell proliferation by about 10%. Based on this observation, the four concentrations, including the highest safe dose (50 μg/ml) were used in subsequent antiviral assays.

3.3. HBsAg inhibitory activity by quercetin and myricetin-3-rhamnoside

The flavonoids quercetin and myricetin-3-*O*-rhamnoside isolated from *G. senegalensis* showed dose-dependent inhibition of HBsAg expressions in relation to untreated control in HepG2.2.2.15 culture supernatants. The estimated HBsAg inhibitions by quercetin and myricetin-3-*O*-rhamnoside were ~60% ($P < 0.001$) and ~44% ($P < 0.01$), respectively at the maximal dose 50 μg/ml at day 3 (Fig. 3).

3.4. Down regulation of HBV replication by quercetin and myricetin-3-O-rhamnoside

Further, the maximal inhibition of HBeAg expressions by 50 μg/ml of quercetin and myricetin-3-*O*-rhamnoside were ~62% ($P < 0.001$) and ~35% ($P < 0.01$), respectively at day 5 (Fig. 4). Notably, quercetin had higher anti-HBV activity, close to that of lamivudine (69%). Because of the cell proliferative activity of the compounds, incubation beyond day 5 resulted in cell overgrowth and death, and therefore, higher time-points were not included (Arbab et al., 2017; Parvez et al., 2019).

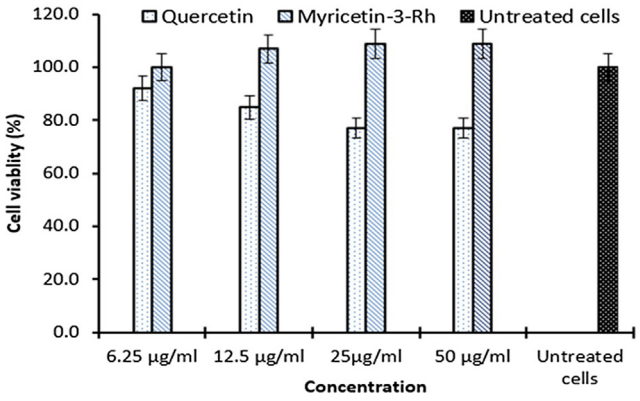

Fig. 2. Effect of *G. senegalensis* derived quercetin and myricetin-3-*O*-rhamnoside on HepG2.2.2.15 cell viability relative to untreated control at day 3 post-treatment. Values on Y-axis are means of three determinations.

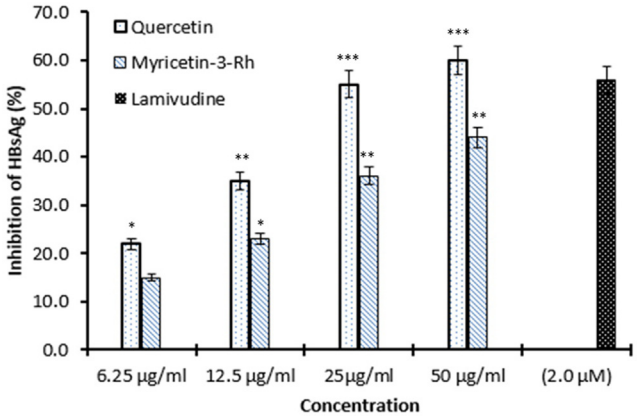

Fig. 3. Inhibition of HBsAg expressions by *G. senegalensis* derived quercetin, myricetin-3-*O*-rhamnoside and lamivudine relative to untreated control in HepG2.2.2.15 culture supernatants at day 3 post-treatment. Values on Y-axis are means of three determinations (*$P < 0.05$, **$P < 0.01$, ***$P < 0.001$).

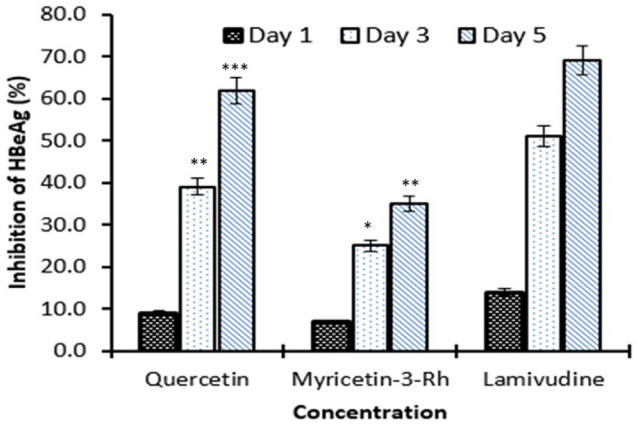

Fig. 4. Inhibition of HBeAg expressions by quercetin, myricetin-3-*O*-rhamnoside, and lamivudine relative to untreated control in HepG2.2.2.15 culture supernatants at day 1, 3 and 5 post-treatment. Values on Y-axis are means of three determinations (*$P < 0.05$, **$P < 0.01$, ***$P < 0.001$).

3.5. Homology modeling and validation

The modeled HBV-Pol/RT (GeneBank no. ADA95798.1) (Fig. 5A) and human NTCP (PDB no. Q14973) (Fig. 5B) validated by Ramachandran plot showed 87.5% and 96.73% of the residues occupying the favored region for Pol/RT and NTCP, respectively where 4.17% and 1.09% of the residues were located in the disallowed outlier region. The remaining percentage of residues occupied the allowed region. The Ramachandran plot therefore, predicted that both constructed models of Pol/RT and NTCP were of good quality to be used for further *in silico* studies.

3.6. Molecular docking

Both myricetin-3-*O*-rhamnoside and quercetin showed good docking scores toward all target proteins. Moreover, they both had better affinities toward viral Pol/RT and Core than standards lamivudine and the ligand HAP, respectively. However, as compared to quercetin, myricetin-3-*O*-rhamnoside had higher affinity

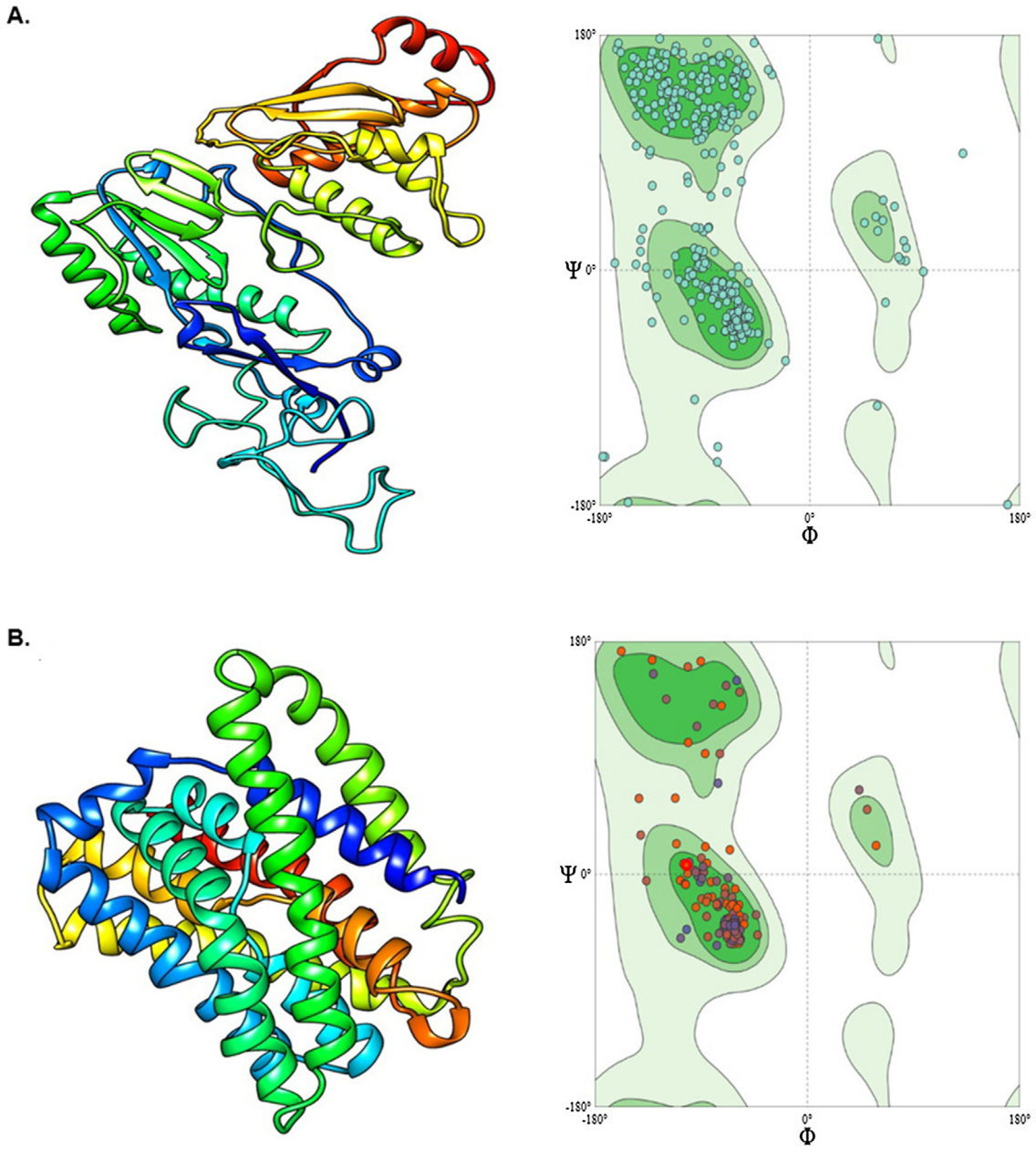

Fig. 5. 3D structure of modeled (A) HBV Pol/RT and Ramachandran plot, and (B) NTCP and Rmachandran plot.

toward all targets except HBV-Core which could be attributed to the hydrogen-bonding potential of the rhamnose moiety (Suppl. materials). As shown in the 2D representation of protein-ligand interactions (Figs. 6–8), both compounds were involved in at least one hydrogen-bonding interaction with the active-site of the targets. They exhibited similar modes of interactions with different residues of active-sites through hydrogen-bonding and hydrophobic contacts owing to their common flavanol skeleton.

The HBV-Pol/RT has been the most targeted viral protein for anti-HBV drugs, notably the NAs (e.g., lamivudine). When docked, both myricetin-3-*O*-rhamnoside and quercetin shared same hydrogen-bond interactions with the modeled Pol/RT Gln104 and Met204 residues (Fig. 6). Interestingly, as compared to the docking score i.e. the minimum binding affinity of lamivudine (E = −5.4 Kcal/mol) towards Pol/RT, both flavonoids showed higher affinities with docking scores of −6.3 and −7.7 Kcal/mol, respectively. Other surrounding residues that also interacted were Pro59 and Ser202 for myricetin-3-*O*-rhamnoside (Fig. 6A), and Lys60 and Ser185 for quercetin (Fig. 6B). In addition, similar to lamivudine, both compounds also shared same hydrogen bonding with Asp552 and Asp429 in coordination with Mg^{2+}. In light of these results, HBV-Pol/RT could be envisioned as potential viral target of myricetin-3-*O*-rhamnoside and quercetin.

In contrast to the other targets in this study, docking of the two *G. senegalensis* derived flavonoids with HBV-Core showed that quercetin had a higher binding affinity than myricetin-3-*O*-rhamnoside (Suppl. materials). Myricetin-3-*O*-rhamnoside showed only hydrogen bonds with Phe23, Thr33, Ser106 and Tyr118, attributed to its weaker binding affinity compared to quercetin (Fig. 7A). On the other hand, quercetin exhibited three sites of contact with Ser106, Thr109 and Leu140 through hydrogen bonding (Fig. 7B). It addition, it also formed a π-π interaction with Phe110 and a hydrophobic contact with Leu140. When docked, HAP showed hydrophobic interactions with HBV-Core Phe23,

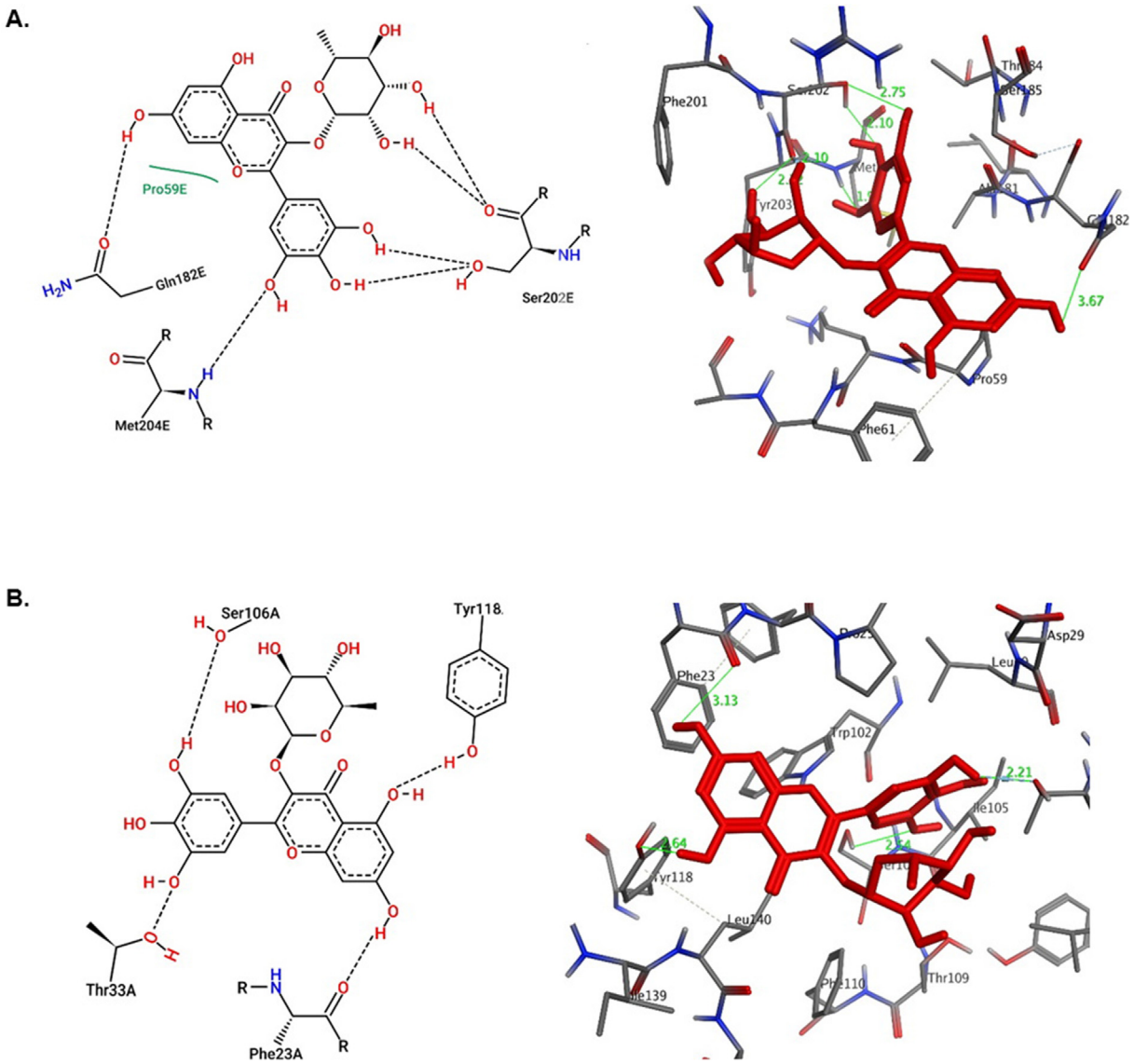

Fig. 6. *In silico* predicted 2D and 3D structures of interactions of HBV-Pol/RT with (A) myricetin-3-*O*-rhamnoside and (B) quercetin.

Pro25, Val124 and Thr128 residues (Fig. 7C) with a binding affinity lower than quercetin and myricetin-3-*O*-rhamnoside, respectively (Suppl. materials).

Docking of NTCP with quercetin and myricetin-3-*O*-rhamnoside showed comparable docking energies −7.4 and −7.6 Kcal/mol, respectively (Suppl. materials). Having common structural features, both compounds interacted similarly with NTCP Gln297 and Gln298 residues through hydrogen bonds (Fig. 8). However, although Thr110 was involved in both cases, it showed hydrophobic interaction with myricetin-3-*O*-rhamnoside (Fig. 8A) whereas formed hydrogen bond with quercetin (Fig. 8B). Both compounds had extra hydrogen bonding with the surrounding amino acid residues.

4. Discussion

Flavonoids (isoflavonoids, flavones, flavanols and anthocyanidins) constitute the largest source of antiviral molecules in the entire plant kingdom (Ono et al., 1990; Vlientinck et al., 1998). In general, flavonoids exist as their glycosides namely, glucosides, galactosides, arabinosides, rutinosides and rhamnosides. Of the several known anti-HBV flavonoids and their phenolic derivatives, wogonin (*Scutellaria radix*) (Cui et al., 2010; Guo et al., 2007), hyperoside (*Abelmoschus manihot*) (Wu et al., 2007), epigallocatechin-3-gallate (*Camellia sinensis*) (He et al., 2011) and ellagic acid (*Phyllanthus urinaria*) (Kang et al., 2006) etc. have been reported as strong inhibitors of HBV markers (HBsAg and HBeAg) in both *in vitro* and *in vivo* models. Notably, while geraniin (*Geranium carolinianum*) is shown more effective than the NA drug lamivudine at same concentration (Li et al., 2008), protocatechuic aldehyde (*Salvia miltiorrhiza*) is a widely accepted traditional Chines medicines for chronic hepatitis B (Zhou et al., 2007). *G. senegalensis* is reported for its antiviral activities against FPV and HSV, from which four flavonoids (quercetin, rutin, myricitrin and catechin) are previously isolated (Bucar et al., 1996; Ficarra et al., 1997; Males et al., 1998). We have recently reported anti-HBV potential of *G. senegalensis* leaves extract and identified quercetin, including seven biomarkers by HPTLC method (Arbab et al., 2017; Alam et al., 2017; Parvez et al., 2018). Very recently, isolation of quercetin and myricetin-3-*O*-rhamnoside along with five polyphenols from *G. senegalensis* is also reported (Dirar et al., 2019). In the present study, we further report bioassay-guided isolation of myricetin-3-*O*-rhamnoside and quercetin as novel anti-HBV active

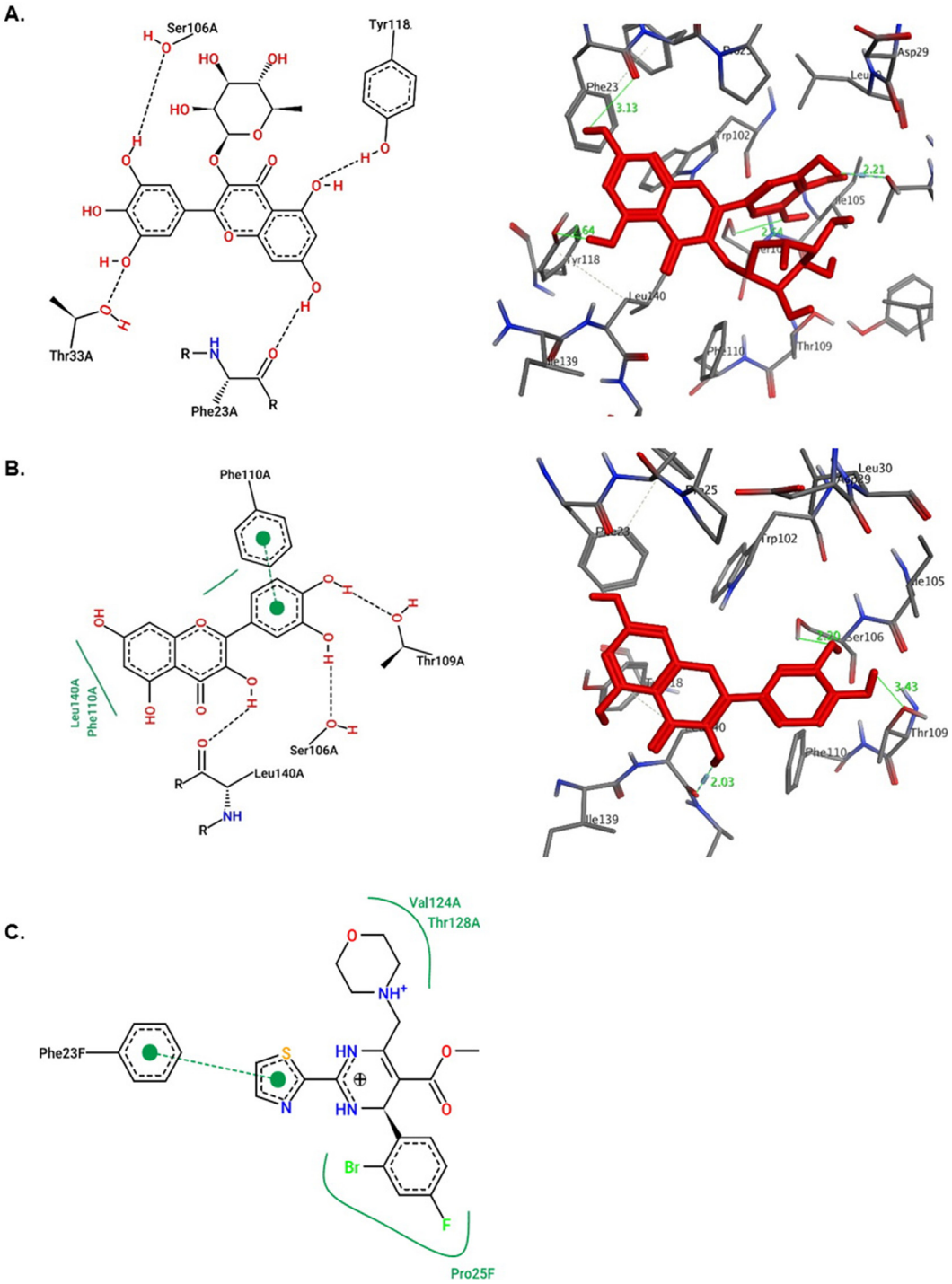

Fig. 7. *In silico* predicted 2D and 3D structures of interactions of HBV-Core with (A) myricetin-3-*O*-rhamnoside and (B) quercetin. (C) 2D representation of HBV-Core and HAP interaction.

principles from *G. senegalensis* leaves *n*-butanol fraction, and predicted their mechanisms of action by molecular docking.

Myricetin is a common flavonoid which occurs as free as well as glycosides *viz.* myricetin-3-*O*-rhamnoside, -arabinopyranoside, -rhamnopyranoside, -galactopyranoside, -xylopyranoside, and -arabinofuranoside (Semwal et al., 2016). Myricetin is structurally related to several well-known flavanols, namely quercetin, morin, kaempferol and fisetin. Notably, at position 3′ of their common structures, while quercetin has an extra substitution with a hydroxy group, myricetin-3-*O*-rhamnoside has this hydroxy group glycosylated with rhamnose moiety. Myricetin is shown to inhibit HIV replication *in vitro* (Pasetto et al., 2014), probably through inactivation of Pol/RT (Ono et al., 1990). Interestingly, the improved anti-HIV activities by the glycosyl moieties of quercetin and myricetin derivatives are also demonstrated (Ortega et al., 2017). In addition, significantly improved anti-HIV and anti-HSV efficacies by 3-*O*-glycosylation of quercetin and myricetin have been reported (Olivero-Verbel and Pacheco-Londoño, 2002; Yarmolinsky et al., 2012). Also, quercetin and myricetin-3-*O*-rhamnoside from *Diospyros lotus* are shown with anti-HIV activi-

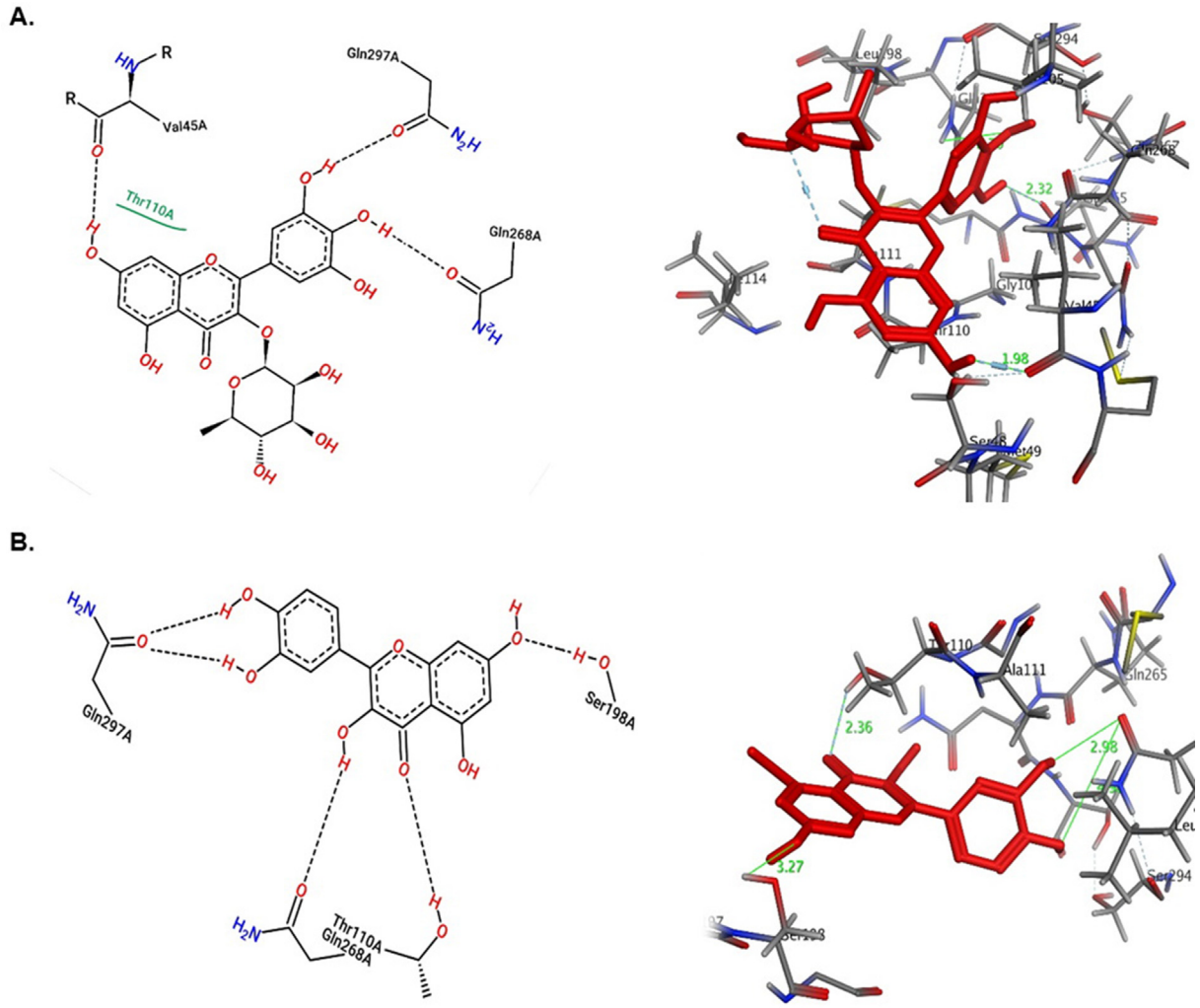

Fig. 8. *In silico* predicted 2D and 3D structures of interactions of NPTC with (A) myricetin-3-*O*-rhamnoside and (B) quercetin.

ties (Rashed et al., 2012). However, myricetin-3-rhamnoside isolated from *Pistacia chinensis* (Rashed et al., 2014) and *Limonium sinense* (Hsu et al., 2015) did not show significant effect on hepatitis C virus (HCV) *in vitro*. While inhibitory effect of quercetin-3-*O*-rhamnoside on influenza A virus replication is shown previously (Choi et al., 2009), very recently, antiviral activity of myricetin-3-*O*-rhamnoside against influenza H1N1 has been reported (Motlhatlego et al., 2018). In line with this, isolation of myricitrin (myricetin-3-*O*-rhamnoside) from *G. senegalensis* (Ficarra et al., 1997) can be attributed to its activities against fowl pox virus and HSV. In this report, our *G. senegalensis* derived myricetin-3-*O*-rhamnoside inhibits HBsAg and HBeAg by 44% and 35%, respectively that is however, lower than that of quercetin. Nonetheless, this is the first report on *in vitro* anti-HBV activity of myricetin-3-*O*-rhamnoside isolated from *G. senegalensis*.

Quercetin is the aglycon form of a number of other flavonoid glycosides, such as rutin. In addition to its several therapeutic values, quercetin is also shown to have *in vitro* activities against mengovirus, HSV virus, parainfluenza virus, pseudorabies virus, respiratory syncytial virus, sindbis virus, HIV and HBV (Wleklik et al., 1998; Kaul et al., 1985; Vrijsen et al., 1988; Choi et al., 2009; Mucsi, 1984; Lamien et al., 2005; Chiow et al., 2016; Cheng et al., 2015). Also, quercetin and structurally related rosmarinic acid are recently shown to inhibit HBV replication through targeting HBV epsilon signal-polymerase interaction in cultured cells (Tsukamoto et al., 2018). Very recently, we have demonstrated the high anti-HBV potential of quercetin that inhibited HBsAg and HBeAg synthesis by 68% and 73%, respectively in cultured HepG2.2.2.15 cells (Parvez et al., 2019). In addition, quercetin when evaluated for additive effects with other tested anti-HBV natural compounds (baccatin III, psoralen, embelin, menisdaurin and azadirachtin) individually, showed enhanced activity by 8–10%. In line with this, our *G. senegalensis* derived quercetin significantly inhibits HBsAg and HBeAg by about 60% and 62%, respectively. Notably, this is the first experimental report on the anti-HBV activity of quercetin isolated from *G. senegalensis* leaves.

Further, to elucidate the anti-HBV modes of action and to determine the molecular interaction patterns, the two compounds were docked with viral Pol/RT and Core proteins as well as a host-encoded receptor NTCP. In our previous study, docking of quercetin with Pol/RT revealed formation of stable bonds, notably with Asp205 of the catalytic motif that stabilized the quercetin-Pol/RT complex with an estimated free energy of −7.4 kcal/mol (Parvez et al., 2019). In the present analysis, both quercetin and myricetin-3-*O*-rhamnoside shows better affinities toward Pol/RT as compared to lamivudine. The HBV-Core protein is considered as a promising viral target for drug development because of its multiple roles in the viral life cycle (Corcuera et al., 2018). Upon docking, Core showed a higher binding affinity with quercetin than myricetin-3-*O*-rhamnoside. HAP represents a novel class of

anti-HBV molecule targeting Core through its HAP pocket (Zhou et al., 2017; Wu et al., 2017). When docked, HAP had however, lower binding affinity than quercetin and myricetin-3-*O*-rhamnoside. Overall, myricetin-3-*O*-rhamnoside was found to have higher affinity toward all targets except HBV-Core. NTCP is a multiple transmembrane transporter predominantly expressed in liver, shown to specifically interact with the receptor-binding region of HBV surface protein (pre-S1). Because silencing of NTCP inhibits HBV infection, it has been further explored as a potential anti-HBV target (Nakabori et al., 2016; Zhang et al., 2015; Yan et al., 2012; Fu et al., 2014). Docking of NTPC protein with quercetin and myricetin-3-*O*-rhamnoside showed their comparable binding-affinities because of common structural features.

5. Conclusion

This is the first report on anti-HBV active myricetin-3-*O*-rhamnoside along with quercetin, isolated from *G. senegalensis* leaves *n*-butanol fraction. Molecular docking of the two anti-HBV flavonoids revealed their higher binding affinities with viral Pol/RT than Core and host NTCP, suggesting possible modes of virus inactivation.

Declaration of Competing Interest

The authors declare that they have no known competing financial interests or personal relationships that could have appeared to influence the work reported in this paper.

Acknowledgment

The authors thankfully acknowledge the Deanship of Scientific Research, King Saud University, Riyadh for funding this work (Project No. RG-1435-053).

Appendix A. Supplementary material

Supplementary data to this article can be found online at https://doi.org/10.1016/j.jsps.2020.03.006.

References

Abubakar, M.S., Sule, M.I., Pateh, U.U., et al., 2000. In vitro snake venom detoxifying action of the leaf extract of Guiera senegalensis. J. Ethnopharmacol. 69, 253–257.

Agrawal, P. K. 1989. Carbon-13 NMR of flavonoids. In: Studies in Organic Chemistry 39. Elsevier.

Akuodor, G.C., Essien, A.D., David-Oku, E., Chilaka, K.C., Akpan, J.L., Ezeokpo, B., Ezeonwumelu, J.O., 2013. Gastroprotective effect of the aqueous leaf extract of Guiera senegalensis in Albino rats. Asian Pac. J. Trop. Med. 6, 771–775.

Alam, P., Parvez, M.K., Arbab, A.H., Al-Dosari, M.S., 2017. Quantitative analysis of rutin, quercetin, naringenin, and gallic acid by validated RP- and NP-HPTLC methods for quality control of anti-HBV active extract of Guiera senegalensis. Pharm. Biol. 55, 1317–1323.

Arbab, A.H., Parvez, M.K., Al-Dosari, M.S., Al-Rehaily, A.J., 2017. In vitro evaluation of novel antiviral activities of 60 medicinal plants extracts against hepatitis B virus. Exp. Ther. Med. 1, 626–634.

Bosisio, E., Mascetti, D., Verotta, L., et al., 1997. Guiera senegalensis JF Gmel (Combretaceae): Biological activities and chemical investigation. Phytomedicine 3, 339–348.

Bouchet, N., Barrier, L., 1998. Fauconneau B. Radical scavenging activity and antioxidant properties of tannins from Guiera senegalensis (Combretaceae). Phytother. Res. 12, 159–162.

Bucar, F., Schubert-Zsilavecz, M., Knauder, E., 1996. Flavonoids of Guiera senegalensis. Pharmazie 51, 517–518.

Cheng, Z., Sun, G., Guo, W., et al., 2015. Inhibition of hepatitis B virus replication by quercetin in human hepatoma cell lines. Virol. Sin. 30, 261–268.

Choi, H.J., Song, J.H., Park, K.S., Kwon, D.H., 2009. Inhibitory effects of quercetin 3-rhamnoside on influenza A virus replication. Eur. J. Pharm. Sci. 37, 329–333.

Corcuera, A., Stolle, K., Hillmer, S., et al., 2018. Novel non-heteroarylpyrimidine (HAP) capsid assembly modifiers have a different mode of action from HAPs in vitro. Antiviral Res. 158, 135–142.

Cui, X., Wang, Y., Kokudo, N., Fang, D., Tang, W., 2010. Traditional Chinese medicine and related active compounds against hepatitis B virus infection. Biosci. Trends. 4, 39–47.

Devi, U., Locarnini, S., 2013. Hepatitis B antivirals and resistance. Curr. Opin. Virol. 3, 495–500.

Dirar, A.B., Adhikari-Devkota, A., Hassan, M.M., Wada, M., Watanabe, T., Devkota, H. P., 2019. Phenolic compounds as potent free radical scavenging and enzyme inhibitory components from the leaves of Guiera senegalensis. Nat. Product Commun. 2019, 1–4.

Ficarra, R., Ficarra, P., Tommasini, S., et al., 1997. Isolation and characterization of Guiera senegalensis J.F.Gmel. active principles. Boll. Chim. Farm. 136, 454–459.

Fu, L.L., Liu, J., Chen, Y., et al., 2014. In silico analysis and experimental validation of azelastine hydrochloride (N4) targeting sodium taurocholate co-transporting polypeptide (NTCP) in HBV therapy. Cell Prolif. 47 (326–335), 2014.

Guo, Q., Zhao, L., You, Q., et al., 2007. Anti-hepatitis B virus activity of wogonin in vitro and in vivo. Antiviral Res. 74, 16–24.

He, W., Li, L.X., Liao, Q.J., Liu, C.L., Chen, X.L., 2011. Epigallocatechin gallate inhibits HBV DNA synthesis in a viral replication-inducible cell line. World J. Gastroenterol. 17, 1507–1514.

Hou, J., Liu, Z., Gu, F., 2005. Epidemiology and Prevention of Hepatitis B Virus Infection. Int. J. Med. Sci. 2, 50–57.

Hsu, W.-C., Chang, S.-P., Lin, L.-W., Li, C.-L., Richardson, C.D., Lin, C.C., Lin, L.T., 2015. Limonium sinense and gallic acid suppress hepatitis C virus infection by blocking early viral entry. Antiviral Res. 118, 139–147.

Kang, E.H., Kown, T.Y., Oh, G.T., et al., 2006. The flavonoid ellagic acid from a medicinal herb inhibits host immune tolerance induced by the hepatitis B virus-e antigen. Antiviral Res. 72, 100–106.

Li, J., Huang, H., Zhou, W., Feng, M., Zhou, P., 2008. Anti-hepatitis B virus activities of Geranium carolinianum L. extracts and identification of the active components. Biol. Pharm. Bull. 31, 743–747.

Males, Z., Medic-Saric, M., Bucar, F., 1998. Flavonoids of Guiera senegalensis J.F. Gmel.-thin-layer chromatography and numerical methods. Croat Chem Acta. 71, 69–79.

MOE. Molecular Operating Environment. 2009. Scientific Comput Instrument. 1, 32–36.

Motlhatlego, K.E., Mehrbod, P., Fotouhi, F., 2018. Antiviral activity against influenza H1N1 virus of myricetin-3- O-rhamnoside isolated from Newtonia buchananii and its mechanism of action. South African J. Botany. 115, 301–306.

Mühlberg, M., Böhrsch, V., Hackenberger, C.P.R., 2009. Chemical biology learning through case studies. In: Waldmann, Herbert, Janning, Petra (Eds.), Angew. Chemie Int. Ed., vol. 48. 8175: 8175.

Nakabori, T., Hikita, H., Murai, K., et al., 2016. Sodium taurocholate cotransporting polypeptide inhibition efficiently blocks hepatitis B virus spread in mice with a humanized liver. Sci. Rep. 6, 27782.

Olivero-Verbel, J., Pacheco-Londoño, L., 2002. Structure–activity relationships for the anti-HIV activity of flavonoids. J. Chem. Inf. Comput. Sci. 42, 1241–1246.

Ono, K., Nakane, H., Fukushima, M., Chermann, J.C., Barré-Sinoussi, F., 1990. Differential inhibitory effects of various flavonoids on the activities of reverse transcriptase and cellular DNA and RNA polymerases. Eur. J. Biochem. 190, 469–476.

Ortega, J.T., Suarez, A.I., Serrano, M.L., Baptista, J., Pujol, F.H., Rangel, H.R., 2017. The role of the glycosyl moiety of myricetin derivatives in anti-HIV-1 activity in vitro. AIDS Res. Ther. 14, 57–62.

Parvez, M.K., Arab, A.H., Al-Dosari, M.S., Al-Rehaily, A.J., 2016. Antiviral natural products against chronic hepatitis B: recent developments. Curr Pharm Des. 3, 286–293.

Parvez, M.K., Alam, P., Arbab, A.H., Al-Dosari, M.S., Alhowiriny, T.A., Alqasoumi, S.I., 2018. Analysis of antioxidative and antiviral biomarkers β-amyrin, β-sitosterol, lupeol, ursolic acid in Guiera senegalensis leaves extract by validated HPTLC methods. Saudi Pharm. J. 2, 685–693.

Parvez, M.K., Rehman, M.T., Alam, P., Al-Dosari, M.S., Alqasoumi, S.I., Alajmi, M.F., 2019. Plant-derived antiviral drugs as novel hepatitis B virus inhibitors: Cell culture and molecular docking study. Saudi Pharm. J. 27, 389–400.

Pasetto, S., Pardi, V., Murata, R.M., 2014. Anti-HIV-1 activity of flavonoid myricetin on HIV-1 infection in a dual-chamber in vitro model. PLoS ONE. 29, e115323.

Rashed, K., Calland, N., Deloison, G., Rouille, Y., Seron, K., 2014. In-vitro antiviral activity of Pistacia chinensis flavonoids against hepatitis C virus (HCV). J. App. Pharm. 6, 8–18.

Rashed, K., Zhang, X.-J., Luo, M.-T., Zheng, Y.-T., 2012. Anti-HIV-1 activity of phenolic compounds isolated from Diospyros lotus fruits. Phytopharmacology 3, 199–207.

Sanogo, R., De Pasquale, R., Germanò, M.P., 1998. The antitussive activity of Guiera senegalensis J.F.Gmel. (Combretaceae). Phytother. Res. 12, 132–134.

Semwal, D.K., Semwal, R.B., Combrinck, S., Viljoen, A., 2016. Myricetin: a dietary molecule with diverse biological activities. Nutrients 8, 90.

Shepard, C.W., Simard, E.P., Finelli, L., Fiore, A.E., Bell, B.P., 2006. Hepatitis B virus infection: epidemiology and vaccination. Epidemiol. Rev. 28, 112–125.

Silva, O., Gomes, E.T., 2003. Guieranone A, a naphthyl butenone from the leaves of Guiera senegalensis with antifungal activity. J. Nat. Prod. 66, 447–449.

Silva, O., Barbosa, A.S., Diniz, A., Valdeira, M.L., Gomes, E., 1997. Plant extracts antiviral activity against Herpes simplex virus type 1 and African swine fever virus. Int. J. Pharmacog. 35, 12–16.

Sombié, P.A.E.D., Hilou, A., Mounier, C., et al., 2011. Antioxidant and anti-inflammatory activities from galls of Guiera senegalensis J.F. Gmel. (Combretaceae). Res. J. Med. Plants. 5, 448–461.

Somboro, K., Patel, D., Diallo, L., et al., 2011. An ethnobotanical and phytochemical study of the African medicinal plant Guiera senegalensis. J. F. Gmel. J. Med. Plants. Res. 5, 1639–1651.
Suleiman, M.H., 2015. An ethnobotanical survey of medicinal plants used by communities of Northern Kordofan region. Sudan. J. Ethnopharmacol. 176, 232–242.
Tang, L.S.Y., Covert, E., Wilson, E., Kottilil, S., 2018. Chronic hepatitis B infection: A review. JAMA 319, 1802–1813.
Trott, O., Olson, A.J., 2010. AutoDock Vina: Improving the Speed and Accuracy of Docking with a New Scoring Function, Efficient Optimization, and Multithreading. J. Comput. Chem. 31, 455–461.
Tsukamoto, Y., Ikeda, S., Uwai, K., et al., 2018. Rosmarinic acid is a novel inhibitor for Hepatitis B virus replication targeting viral epsilon RNA-polymerase interaction. PLoS One. 13, e0197664.
Vlietinck, A.J., Vanden, D.A., Haemers, A., 1998. Present status and prospects of flavonoids as anti-viral agents. Prog. Clin. Biol. Res. 280, 283–299.
Wang, G., Zhang, L., Bonkovsky, H.L., 2012. Chinese medicine for treatment of chronic hepatitis B. Chin. J. Integr. Med. 18, 53–55.
Waterhouse, A. et al., 2018. SWISS-MODEL: homology modelling of protein structures and complexes. Nucl. Acids Res. 46, W296–W303.
Wu, L.L., Yang, X.B., Huang, Z.M., Liu, H.Z., Wu, G.X., 2007. In vivo and in vitro antiviral activity of hyperoside extracted from Abelmoschus manihot (L) medik. Acta Pharmacol. Sin. 28, 404–409.
Wu, Y.H., 2016. Naturally derived anti-hepatitis B virus agents and their mechanism of action. World J. Gastroenterol. 22, 188–204.
Yan, H., Zhong, G., Xu, G., et al., 2012. Sodium taurocholate cotransporting polypeptide is a functional receptor for human hepatitis B and D virus. Elife 1, e00049.
Yarmolinsky, L., Huleihel, M., Zaccai, M., Ben-Shabat, S., 2012. Potent antiviral flavone glycosides from Ficus benjamina leaves. Fitoterapia 83, 362–367.
Zhang, J., Fu, L.L., Tian, M., et al., 2015. Design and synthesis of a novel candidate compound NTI-007 targeting sodium taurocholate cotransporting polypeptide [NTCP]–APOA1–HBx–Beclin1-mediated autophagic pathway in HBV therapy. Bioorg. Med. Chem. 23, 976–984.
Zhou, Z., Hu, T., Zhou, X., et al., 2017. Heteroaryldihydropyrimidine (HAP) and Sulfamoylbenzamide (SBA) inhibit hepatitis B virus replication by different molecular mechanisms. Sci. Rep. 7, 42374.
Zhou, Z., Zhang, Y., Ding, X.R., et al., 2007. Protocatechuic aldehyde inhibits hepatitis B virus replication both in vitro and in vivo. Antiviral Res. 74, 59–64.